



Experimental verification of near-field lattice spectroscopy

Pin Han¹ · Hsun-Ching Hsu¹ · Hsu-Wen Cheng¹ · Tsung-Han Hsieh¹ · Cheng-Ling Lee² · Hung-Bin Lee³

Received: 2 May 2019 / Accepted: 20 July 2019
© Springer-Verlag GmbH Germany, part of Springer Nature 2019

Abstract

Near-field lattice spectroscopy has shown that the structure information for a lattice or periodic pattern can be obtained by measuring the diffracted spectrum of a broad-band light source at one spatial position. This technique is verified experimentally using a transmitting grating, supercontinuum white light laser, and a reflective concave mirror. The calculated grating's period from the detected lattice spectroscopy is close to the measured period with an optical microscope, which demonstrates the validity and feasibility of this scheme.

1 Introduction

The deciding of parameters for periodic configurations, such as a grating or crystal lattice, is of important in measurement science. For examples, the 2-D grating projection is used to determine the 3-D profile (Su and Zhang 2010), periodic photonic crystal fibers for optical sensing (Frazao et al. 2009), and diffraction grating for displacement measurement (Lu et al. 2016). There are many traditional ways to determine the period of the objects, for examples, direct measurement with optical microscope, or indirect one like the X-ray crystallography (Keen 2014) obtaining the period from the monochromatic diffraction pattern from the crystal lattice.

Recently a spatial-spectral correspondence relationship for mono-poly chromatic light diffraction was proposed by the author (Han 2018). It states that in the domain of paraxial region (i.e. where the Fresnel (near-field) approximation or Fraunhofer (far-field) approximation can be applied), the spatial distribution of mono-chromatic light diffraction corresponds to the spectral distribution of poly-chromatic light, under the condition that the incident light is fully spatially coherent and completely position

independent in the structure region causing the diffraction. This relationship has been applied successfully and many important results or interesting effects were found, such as the lattice spectroscopy, Talbot spectrum (Han 2015), Fresnel zone spectrum (Su and Zhang 2010), absolute range finder (Hsieh and Han 2018; <https://www.keyence.com/products/measure/spectral/si-f/index.jsp>; Wu et al. 2016) and spectral switches (Pu et al. 1999; Kandpal 2001). The far-field lattice spectroscopy (Han 2009) is about determining the structure of a periodic aperture (such as a grating) by detecting the diffracted polychromatic spectrum at an arbitrary position, instead of recording the monochromatic diffraction pattern with a photographic plate or a sensor moving around in the space; the latter is usually applied in crystallography and maybe more time-consuming. To improve the convenience and utilization of this method, the author suggested the near-field lattice spectroscopy scheme (Han 2011), with which the diffracted spectrum is measured at a focal plane of a convergent mirror; consequently the needed space is reduced substantially. In this work, an experiment is performed to verify the theoretical prediction; we find that the experimental results agree well with the theoretical ones. In the following, we will give the complete setup of the experiment and explain the measured data in detail. This article is organized as the following: First the introduction presents the historic review and motives for the work. Next we illustrate the measurement principle and derive the equations that will be used later for the calculations. Then an experiment is executed to obtain the spectrum and it is compared with the theoretic calculations. Finally we made some conclusions and discussions.

✉ Hung-Bin Lee
lhb6018@mail.ntou.edu.tw

¹ Graduate Institute of Precision Engineering, National Chung Hsing University, Taichung 402, Taiwan

² Department of Electro-Optical Engineering, National United University, Miaoli 360, Taiwan

³ Department of Optoelectronics and Materials Technology, National Taiwan Ocean University, Keelung 202, Taiwan

2 Measurement principle

The complete theory is described in the previous article (Han 2011); thus we will just briefly review it here. Considering Fig. 1a, a one-dimensional transmission grating with the following parameters: a is the width of transparent part (white area in the figure), b is the period (one opaque (shaded area) and one transparent stripe), and d is the total width that is used by the incident light, which is usually controlled by an adjustable iris that the incident light goes through. This grating is placed at the aperture plane ($z = z_1$), as shown in Fig. 1b; at distance l behind it a concave mirror is placed at ($z = z_2$) with reflectivity $R(\omega)$ and focal length f_c , where ω is the angular frequency of the incident light. In free space it is related to the wavelength λ with the relation $\omega = 2\pi c/\lambda$, c being the speed of light. In the following we will use ω or λ interchangeably to represent the spectral variable. Note that here the converging element is a mirror, instead of a lens, because the latter results in a wavelength dependent focal length (due to the material dispersion) for polychromatic light, which is not desirable in this scheme.

Now a uniformly distributed and spatially fully coherent broadband light with spectrum $S_1(\omega)$ is incident into the grating at $z = z_1$; it is first diffracted by the grating and then reflected by the mirror. If a spectrum detector is placed at a point P in the focal plane ($z = z_3$, which is in front of the mirror with distance f_c) with vertical distance x_3 (see Fig. 1b), the detected spectrum with spectral variables ω or λ at P are:

$$S(P, \omega) \propto \omega^2 \cdot R(\omega) \cdot |F[g(x_1)]|^2 \cdot S_1(\omega) \tag{1a}$$

$$S(P, \lambda) \propto \omega^2 \cdot R(\lambda) \cdot |F[g(x_1)]|^2 \cdot S_1(\lambda), \tag{1b}$$

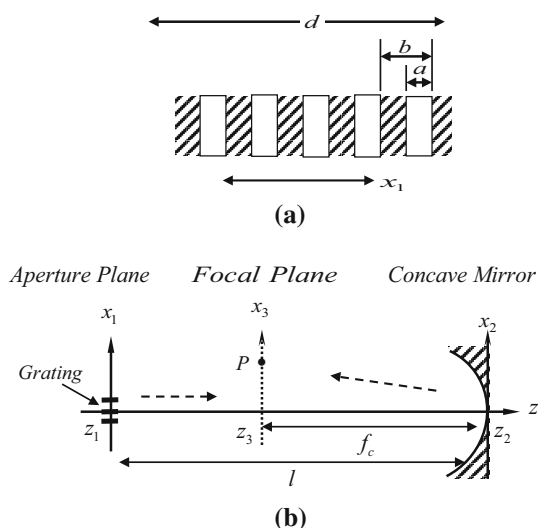


Fig. 1 a Schematic plot of a transmission grating. b The schematic configuration of the near-field lattice spectroscopy

where $F[g(x_1)]$ is the Fourier transform of the grating with the spatial frequency $f_x = x_3/\lambda f_c = \omega \cdot x_3/2\pi c f_c$. The aperture function of the grating in Fig. 1a is (Iizuka 1983).

$$g(x_1) = \frac{1}{b} \left[\text{rect} \left(\frac{x_1}{a} \right) * \text{comb} \left(\frac{x_1}{b} \right) \right] \cdot \text{rect} \left(\frac{x_1}{d} \right), \tag{2}$$

where $\text{rect}(x'/a)$ is the rectangular function defined as $\text{rect}(x'/a) = 1$ for $|x'| \leq a/2$ and $\text{rect}(x'/a) = 0$ for $|x'| > a/2$, $\text{comb}(x'/b)$ is the comb function defined as $\text{comb}x'/b = b \sum_{n=-\infty}^{\infty} \delta(x' - bn)$, and the symbol $*$ is the convolution operation. From Eq. (2), under the condition $d \gg a, b$, we have

$$|F[g(x_1)]|^2 \propto \{ \text{sinc}(\pi a f_x) \cdot [\text{comb}(b f_x) * \text{sinc}(\pi d f_x)] \}^2, \tag{3}$$

where $\text{sinc}(x)$ is the sinc function defined as $\text{sinc}(x) = \sin(x)/x$. Substituting Eq. (3) into Eq. (1), the diffraction spectrum $S(P, \omega)$ is obtained, if $R(\omega)$ and $S_1(\omega)$ are given. Figure 2 illustrates a typical normalized $S(P, \omega)$, where an assumed flat function of $R(\omega)$ and $S_1(\omega)$ are used. Note that the variable $f_x = x_3/\lambda f_c = \omega \cdot x_3/2\pi c f_c$ in the abscissa is a spectral variable because x_3 and f_c are set. From Fig. 2 we see that if the diffracted is measured, one or even all of the grating parameters (such as a , b , and d in Fig. 1a) can be inferred. Usually the most concerned parameter is the period b of the grating, which can be decided by taking the spectral distance of the two spikes, as shown in Fig. 2, and it will be illustrated below.

Note that the focal length of the mirror should be in the near-field region because Eq. (1) is derived from the near-field approximation.

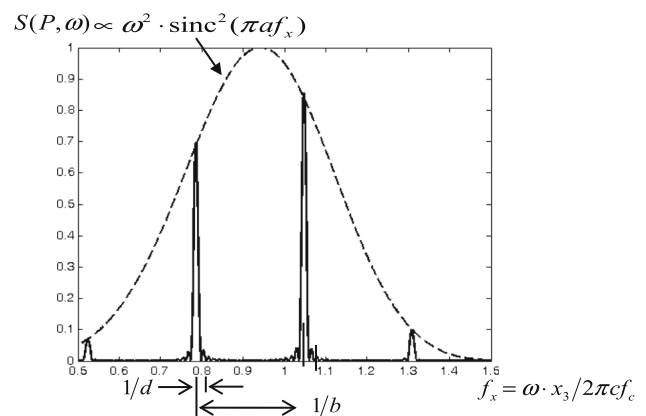


Fig. 2 A typical near-field lattice spectrum of a period configuration as in Fig. 1a

3 Experimental setup and results

As mentioned above, the grating period can be obtained by either recording the diffraction pattern of quasi-monochromatic light or measuring the diffraction spectrum of polychromatic light. We will do both. A transmission grating is made with a Laser Pattern Generator (HIMT DWL_2.0). The designed parameters are set with $a = 3.0 \mu\text{m}$ and $b = 6.0 \mu\text{m}$; however, because of the fabrication error, after it is made and measured with an optical microscope equipped with length measurement function, the measured widths are $a = 3.42 \mu\text{m}$ and $b = 6.15 \mu\text{m}$, as shown in Fig. 3a. The quasi-monochromatic light diffraction is checked first. The setup is shown in Fig. 3b, where a supercontinuum white light laser (NKT-super compact model) beam is filtered by a narrow band pass filter (center wavelength 634 nm and band width 5 nm) to give quasi-monochromatic light. Then it is expanded with a beam expander that consists of a microscope objective lens and a double convex lens. A 2-mm diameter beam is acquired with an adjustable iris and it is incident onto the grating. A lens with focal length $l = 40 \text{ cm}$ is used to bring the far-field diffraction pattern onto the focal plane; as shown in Fig. 3c, the diffraction

pattern with different orders are clearly seen on the plane. The diffraction angle θ_m can be obtained by measuring the longitudinal distance z and transversal one x with $\theta_m = \tan^{-1}(x_m/l)$, as in Fig. 3d. Table 1 shows the measured data and calculations. The calculated period b in last column using the following grating equation (Hecht 2002):

$$b \cdot \sin(\theta_m) = m \cdot \lambda, \quad m = 0, \pm 1, \pm 2, \dots, \quad (4)$$

where θ_m is the diffraction angle, m the order, and center wavelength 634 nm is used as the λ . It is found that the calculated periods agree well with the measured period $6.15 \mu\text{m}$ in Fig. 3a, and the errors are less than 5%.

Next we check the near-field lattice spectroscopy. The real and schematic setup is illustrated in Fig. 4a, b, respectively, which is similar to Fig. 3b, with the following differences: 1—the narrow band pass filter is removed. The needed fully spatially coherent and uniformly-distributed polychromatic light can be provided with the beam expander and the suitable beam size set by the controllable iris. 2—This collimated polychromatic light beam is diffracted by the grating, as shown in Fig. 4b, and different orders rainbow-like bands, due to the broadband property of the light, are found in the image plane, see Fig. 4c. Note that only two negative orders and one positive order beams

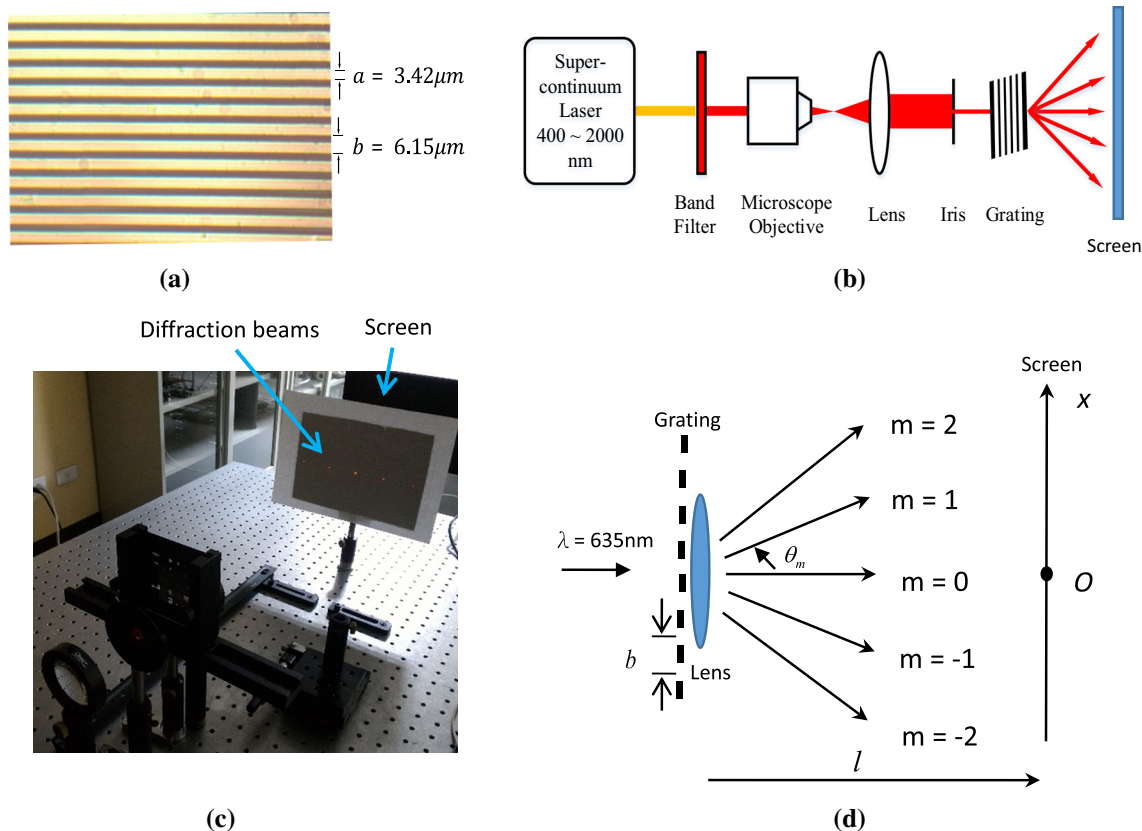


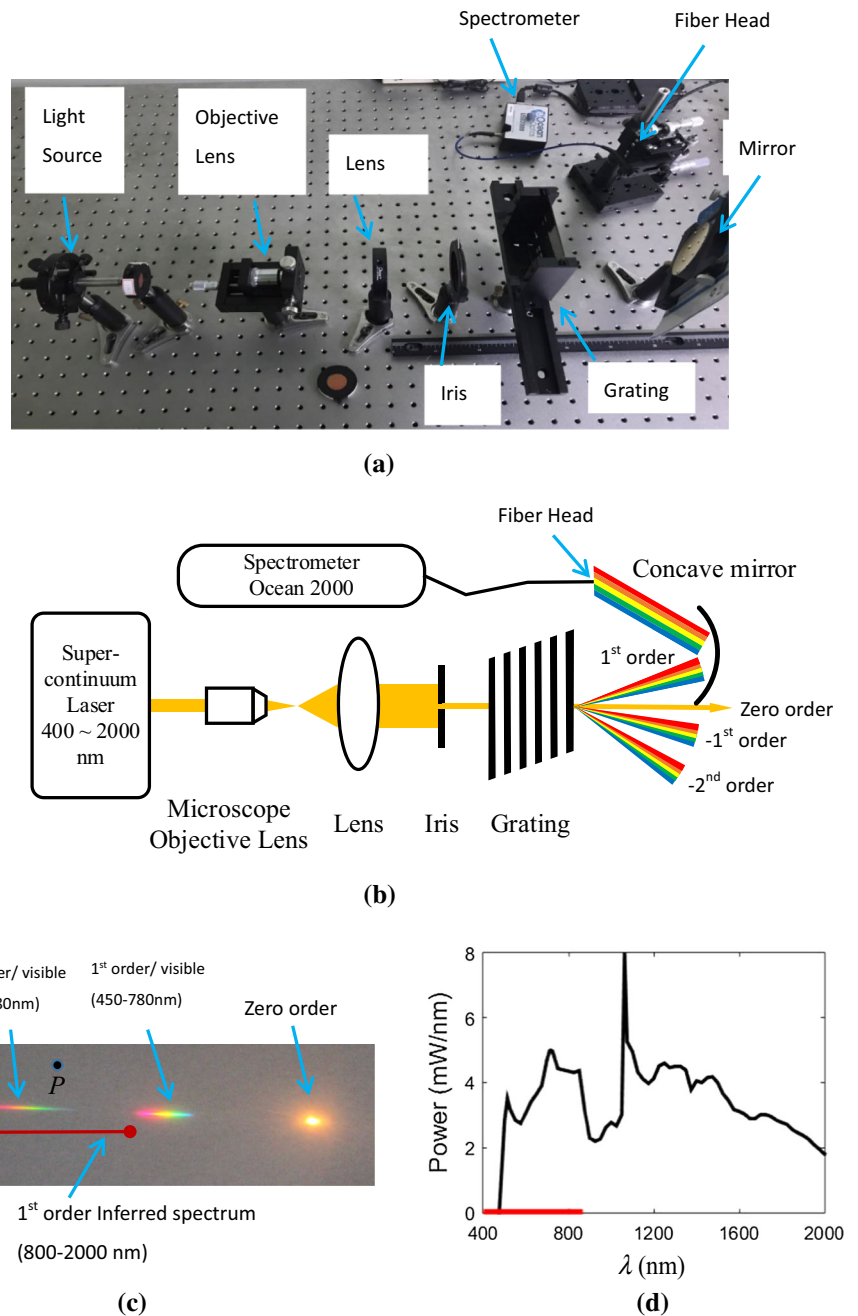
Fig. 3 a The grating sample and its parameters. b The schematic setup. c The diffracted quasi-monochromatic beams. d The schematic plot for grating diffraction

Table 1 Measured data for diffraction beams and calculations for period

m_{th} order	x (cm)	θ_m ($^\circ$)	Calculated period b (μm) with Eq. (4)
1	4.24	6.05	6.02
2	8.55	12.06	6.07
3	12.98	17.98	6.16
4	17.93	24.14	6.20
5	23.44	30.37	6.27

are drawn schematically in Fig. 4b; actually the number of bands are symmetric to the zero order and depend on the period of the grating. Only the visible part of the spectrum for zero and positive beams are photographed with common camera, as indicated in Fig. 4c. Actually the source has much wider spectrum from 0.45 to 2.0 μm , as shown in Fig. 4d, which is $S_1(\lambda)$ in Eq. (1); thus there are infrared spectrum following the rainbow band, as denoted by a dark-red line in Fig. 4c. 3—A 10-cm diameter gold-coated concave spherical mirror with focal length $f_c = 16$ cm is

Fig. 4 **a** The real experimental setup for the near-field lattice spectroscopy. **b** The schematic setup. **c** The diffracted polychromatic spectra. **d** The spectrum of the super continuum laser and detection range of fiber spectrometer (the red line on the abscissa)



placed in front of the grating to focus the diffraction light onto the focal plane, as shown in Fig. 4c. The reflectivity of gold is plotted in Fig. 5a, which is the $R(\lambda)$ in Eq. (1), and it offers good reflectivity for wavelength larger than 460 nm.

The diffracted spectrum at the focal plane is detected by a fiber spectrometer (Ocean USB2000) with a 10 μm opening at the fiber end, as shown in Fig. 4a, b. The spectrometer's response in 400–1050 nm range, as indicated by the red line in the abscissa of Fig. 4d. A typical diffracted spectrum is shown at Fig. 5b, where two spikes similar to Fig. 2 are observed; the number on the top of each spike indicates the peak wavelength. In the following we will interpret the relation in Fig. 2 (i.e. the spatial frequency distance between two adjacent spikes is $1/b$), and explain how to decide the period b by measuring the diffracted spectrum. To facilitate interpreting, the grating diffraction part of Fig. 4b is redrawn as Fig. 6. Referring to Fig. 6, the diffracted spectrum is detected by a fiber spectrometer at P at the focal plane of the mirror ($z = f_c$), where the vertical distance to the center line of the mirror is x_3 . Now considering that one of the wavelength components in the first order beam, say λ_1 , is diffracted into the angle θ_1 , satisfying Eq. (4), $b \cdot \sin(\theta_1) = \lambda_1$, with $m = 1$. However, we note that $b \cdot \sin(\theta_1) = \lambda_1 = 2 \cdot (\lambda_1/2) = 3 \cdot (\lambda_1/3)$, indicating that the second order of $(\lambda_1/2)$ is also diffracted into this angle, as well as the third order of $\lambda_1/3$, etc. Consequently these wavelength beams are focused by the concave mirror and detected by the fiber spectrometer with its fiber head set at the reflection angle θ_1 , as shown in Fig. 6. That is exactly why we can see several spikes in the detected spectrum in Fig. 2; they should be related by the orders $(\lambda_1, \lambda_1/2, \lambda_1/3 \dots)$ and their spectral distance should be $1/b$, as denoted in Fig. 2. This two spikes feature can be observed in Fig. 5(b), which is the diffracted spectrum taken at point P in Fig. 4c. From Fig. 4c, we see that at P the infrared spectrum of the first order is overlapped with second order of the visible spectrum (In Fig. 4c, for the purpose of clarity, we denoted the infrared

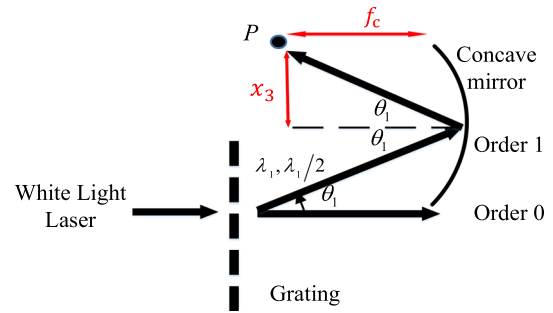


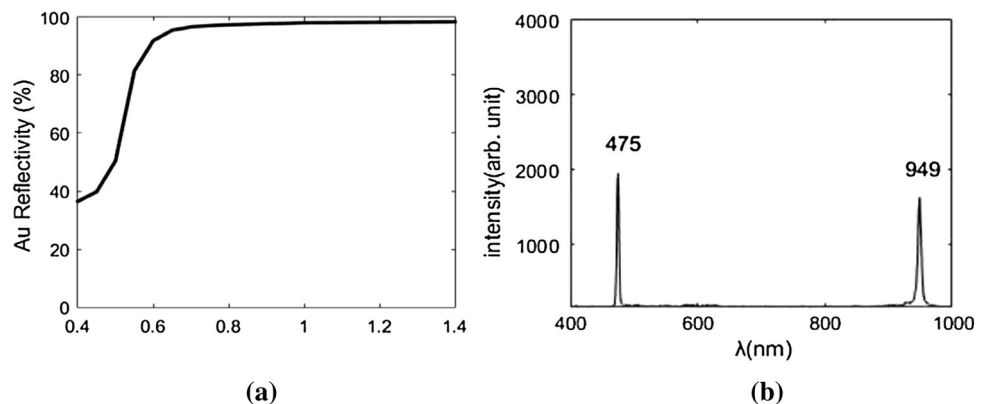
Fig. 6 Schematic plot and notations for interpretation of acquiring period b

spectrum of the first order below the visible spectrum; actually they are at the same level.) Thus both of the peak wavelengths (949 and 475 nm) are detected at P , as in Fig. 5b.

Now the relation that the distance between two adjacent spatial frequencies is b as in Fig. 2(b) can be explained as the following. If two adjacent spectral components λ_1 , and $\lambda_2 \simeq \lambda_1/2$ are detected at some position P as in Fig. 5b, each should correspond to spatial frequency $f_1 = x_3/\lambda_1 f_c$ and $f_2 = x_3/\lambda_2 f_c = 2x_3/\lambda_1 f_c = 2f_1$ respectively, leading to $f_2 - f_1 = x_3/\lambda_1 f_c = \tan(\theta_1)/\lambda_1$. Using the small angle approximation $\tan(\theta_1) \sim \sin(\theta_1)$ and grating equation $b \cdot \sin(\theta_1) = \lambda_1$, above equation can be reduced to $f_2 - f_1 = x_3/\lambda_1 f_c \sim \sin(\theta_1)/\lambda_1 \sim 1/b$. In other words, for spikes come in the order $(\lambda_1, \lambda_1/2, \lambda_1/3 \dots)$, their spatial frequencies are $(1/b, 2/b, 3/b \dots)$. Consequently the spectral distance between any two adjacent spikes is $1/b$, as indicated in Fig. 2b.

Note that because the limited detection range of the fiber spectrometer as in Fig. 4d, at most two spectral spikes can be obtained in the diffracted spectra. In the following the procedures to determine the period b are described and they can be readily generalized to more than two spikes situation. First the setup is built as in Fig. 4a; the fiber head is placed at arbitrary position P on the focal plane of the mirror. Second, we measure the diffracted spectrum and

Fig. 5 a The reflectivity of Au. b Diffracted spectrum at $x_3 = 2.54 \text{ cm}$



take the peak wavelengths λ_1 and λ_2 in the decreasing order; that means λ_1 is the peak with longer wavelength. Third, we measure the vertical distance x_3 from P to the center of the mirror (horizontal dash line), as in Fig. 6. Thus the diffraction angle for λ_1 can be calculated as $\theta_1 = \tan^{-1}(x_3/f_c)$ with $f_c = 16$ cm. Figure 7a–d show the diffracted spectrum at different increasing x_3 values: (a) 2.50 cm (b) 2.54 cm (c) 2.59 cm (d) 2.63 cm. Note that the peak wavelengths denoted on each peak are round-off values to the closest integers, the exact values are given in Table 2. It is found that λ_2 is about half of λ_1 , as expected. Forth, substitute values in Table 2 into the following equation

$$\sin(\theta_1) \left(\frac{1}{\lambda_2} - \frac{1}{\lambda_1} \right) = \frac{1}{b} \quad (5)$$

to obtain the unknown period b . The calculated values of b are also close to the measured one in grating mask (see Fig. 3a with $b = 6.15$ μm). The error is about ± 0.5 μm (about 8%), which is a little greater than the values calculated with monochromatic method, as in Table 1. Note that only two spikes are taken in the diffracted spectrum because of the limited range for the overlap of light source bandwidth and the spectrometer detection bandwidth (about 460–1050 nm).

Fig. 7 Spectra at different x_3 values. **a** 2.50 cm, **b** 2.54 cm, **c** 2.59 cm, **d** 2.63 cm

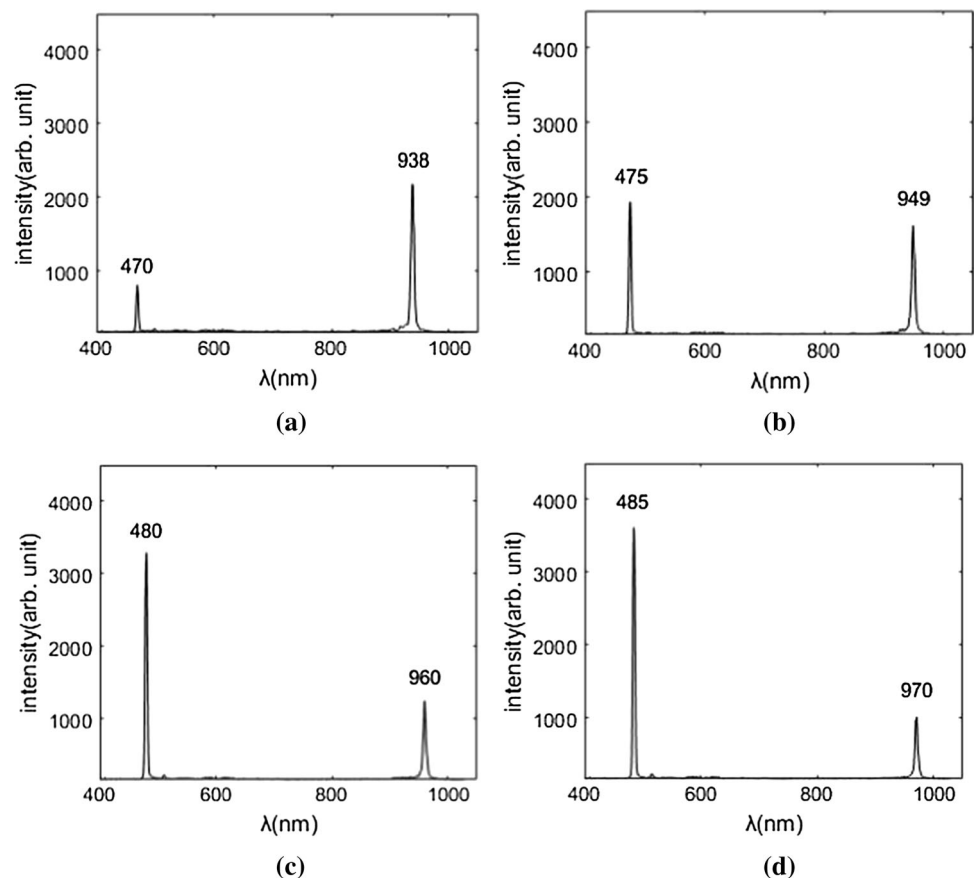


Table 2 Measured data and calculations for b

x_3 (cm)	$\theta(^{\circ})$	λ_1 (nm)	λ_2 (nm)	b (μm)
2.46	8.743	939.18	470.05	6.192
2.52	8.95	949.03	475.29	6.143
2.56	9.09	960.06	480.82	6.182
2.60	9.21	970.74	485.13	6.065

4 Discussion and conclusion

In this work the near-field lattice spectroscopy is verified by experiments. The theory is introduced and interpreted by the grating equation. Both the monochromatic and polychromatic light beam are used to test the validity of the theory. A specific grating made by laser pattern generation and the wide-band supercontinuum laser are used to perform the experiment. The diffracted spectrum (450–2500 nm) is measured by an optical fiber spectrometer which can only respond part of the light source spectrum (400–1050 nm). Consequently, only two spikes can be obtained in the diffracted spectrum, as seen in Fig. 7. If more spikes can be detected and the absolute intensities are obtained, the parameter a (the transparent width as in

Fig. 1a) can be inferred, as denoted in Fig. 2. The parameter d (the beam size transmitting the grating) can also be inferred as follows. From Fig. 2 we know that the spectral width of the spike with peak wavelength λ is $1/d = \Delta f_x \sim \Delta \lambda x_3 / \lambda^2 f_c \sim (\Delta \lambda / \lambda^2) \tan \theta$, which can be derived by differentiating $f_x = x_3 / \lambda f_c$ with λ . Taking the Fig. 7c as the example, the spectral width is about 2 nm for 480.82 nm spike and $\theta = 9.09^\circ$ the calculated $d = \lambda^2 / \Delta \lambda \cdot \tan \theta$ is about 0.8 mm, which is acceptable, compared with the real beam size 1.2 mm. In this experiment, several factors could contribute the errors, including the resolution of the spectrometer, the uncertainties of positions or angles. The aperture size of the fiber head should be considered, because, in principle, the opening of the head should be infinitely small to receive the spectral component at position P . Finite size opening will catch more spectral components, leading to wider bandwidth; thus the error in deciding parameter d using bandwidth is bigger. However, finite aperture would not affect much in deciding peak wavelength and that is probably the reason why the error is not that large in finding parameter b . Also note that this near-field lattice spectroscopy is for polychromatic light, under the condition that the incident light is fully spatially coherent and completely position independent in the structure region causing the diffraction. Thus there should be enough grating's periods in this polychromatic coherent region to obtain the spikes in Fig. 2. Since the coherent and uniform region is in the order of millimeter, if we require at least 10 periods existing in this region, the biggest period of the grating is in the order of 100 μm .

It is believed that this near-field lattice spectroscopy technique is of value in determining the period of periodic structures, such as a grating. Compared with the traditional method recording the monochromatic diffraction pattern, the advantages on space and speed are obvious. It is believed that this new method will find many applications in metrology and spectroscopy.

Acknowledgements This study was supported by the National Chung Hsing University and National Taiwan Ocean University, Taiwan,

R.O.C. The author also would like to thank his colleagues for useful suggestions. This work was also supported by the Ministry of Science and Technology of R.O.C. under contract Nos. MOST-104-2221-E-005-069-MY3, MOST-106-2622-E-005-007-CC3 and MOST 107-2622-E-019-004 -CC3.

References

- Frazao O, Santos JL, Araujo FM, Ferreira LA (2009) Optical sensing with photonic crystal fibers. *Laser Photonics Rev* 2:449–459
- Han P (2015) Spectra restoration of a transmissive periodic structure in near-field diffraction (Talbot Spectra). *J Opt Soc Am A* 32:1076–1083
- Han P (2018) Spatial–spectral correspondence relationship for monochromatic light diffraction. In: Visser TD (ed) *Progress in optics*, vol 63. Elsevier, Amsterdam, pp 33–87 (ISBN: 978-0-444-64117-5)
- Hsieh TH, Han P (2018) Using interference spectrum as short-range absolute rangefinder with fiber and wideband source. *Meas Sci Technol* 29:065006. <https://doi.org/10.1088/1361-6501/aab13f>
- Keen DA (2014) Crystallography and physics. *Phys Scr* 89:128003
- Lu Z, Wei P, Wang C, Jing J, Tan J, Zhao X (2016) Two-degree-of-freedom displacement measurement system based on double diffraction gratings. *Meas Sci Technol* 27:074012
- Su XY, Zhang QC (2010) Dynamic 3-D shape measurement method: a review. *Opt Lasers Eng* 48:191–204
- Available at: <https://www.keyence.com/products/measure/spectral/si-f/index.jsp>. Accessed 11 June 2019
- Han P (2009) Lattice spectroscopy. *Opt Lett* 34:1303–1305
- Han P (2011) Near field lattice spectroscopy with a reflective confocal configuration. *Appl Phys Express* 4:022401
- Hecht E (2002) *Optics*, 4th edn. Addison Wesley, San Francisco, p 477
- Iizuka K: *Engineering Optics* (Kyoritsu Shuppan, Tokyo, 1983) 2nd ed. p 87
- Kandpal HC (2001) Experimental observation of the phenomenon of spectral switch. *J Opt A: Pure Appl Opt* 3:296–299
- Pu J, Zhang H, Nemoto S (1999) Spectral shifts and spectral switches of partially coherent light passing through an aperture. *Opt Commun* 162:57–63
- Wu H, Zhang F, Meng F, Liu T, Li J, Pan L, Qu X (2016) Absolute distance measurement in a combined dispersive interferometer using a femtosecond pulse laser *Meas. Sci Technol* 27(015202):12

Publisher's Note Springer Nature remains neutral with regard to jurisdictional claims in published maps and institutional affiliations.